LETTER

doi:10.1038/nature10565

An impact-driven dynamo for the early Moon

M. Le Bars[1], M. A. Wieczorek[2], Ö. Karatekin[3], D. Cébron[1] & M. Laneuville[2]

The origin of lunar magnetic anomalies[1–5] remains unresolved after their discovery more than four decades ago. A commonly invoked hypothesis is that the Moon might once have possessed a thermally driven core dynamo[3], but this theory is problematical given the small size of the core and the required surface magnetic field strengths[6]. An alternative hypothesis is that impact events might have amplified ambient fields near the antipodes of the largest basins[7], but many magnetic anomalies exist that are not associated with basin antipodes. Here we propose a new model for magnetic field generation, in which dynamo action comes from impact-induced changes in the Moon's rotation rate. Basin-forming impact events are energetic enough to have unlocked the Moon from synchronous rotation[8], and we demonstrate that the subsequent large-scale fluid flows in the core, excited by the tidal distortion of the core–mantle boundary[9], could have powered a lunar dynamo. Predicted surface magnetic field strengths are on the order of several microteslas, consistent with palaeomagnetic measurements[5], and the duration of these fields is sufficient to explain the central magnetic anomalies associated with several large impact basins.

Magnetic field measurements of the Moon from orbit demonstrate that portions of its crust are strongly magnetized[1], and palaeomagnetic analyses of lunar rocks show that some samples possess stable remanent magnetizations[2]. However, the origin of the fields that magnetized the crust and the manner by which the surface field strength varied with time are still being debated[3–5]. Two facts lead us to propose a new model for lunar magnetic field generation, in which a global field is generated by a core dynamo that is powered by changes in the Moon's rotation rate following large impact events. The first observation is that six large impact basins of Nectarian age (which are more than about 4 billion years old) possess central magnetic anomalies[10,11] (Fig. 1 and Supplementary Fig. 1). These basins represent the clearest examples of areas in which endogenous lunar features correlate with magnetic anomalies, and for that reason offer an invaluable clue to the origin of lunar magnetism. It is improbable that these magnetic anomalies are caused by the mare basaltic lava flows present in these basins, because the mare basalts are only weakly magnetic[2] and similarly aged basalts elsewhere on the Moon do not possess magnetic anomalies. Impact cratering studies predict these events to have melted substantial quantities of both the crust and the projectile, forming impact melt sheets several kilometres thick[12]. Lunar impact melt rocks are by far the most magnetic igneous rocks on the Moon[2], and the central magnetic anomalies associated with the Nectarian-age basins most plausibly formed as their melt sheets cooled through their Curie temperatures in the presence of a magnetic field. Given the large conductive cooling timescales of these thick deposits, a stable magnetic field must have been present for thousands of years immediately following the impact event (Supplementary Information, section 4, and Supplementary Fig. 10), and the only plausible means of generating such a field is a core dynamo.

The second fact that bears on the origin of impact-basin-related magnetic anomalies is that each of the corresponding impact events would have significantly affected the rotational state of the Moon, either by unlocking it from synchronous rotation (Supplementary Information, section 3.1, and Supplementary Fig. 3) or by setting up large-amplitude free librations[8] (Supplementary Information, section 3.2). The rotation rate of the solid portion of the Moon would have been instantaneously modified following these impacts, but its molten

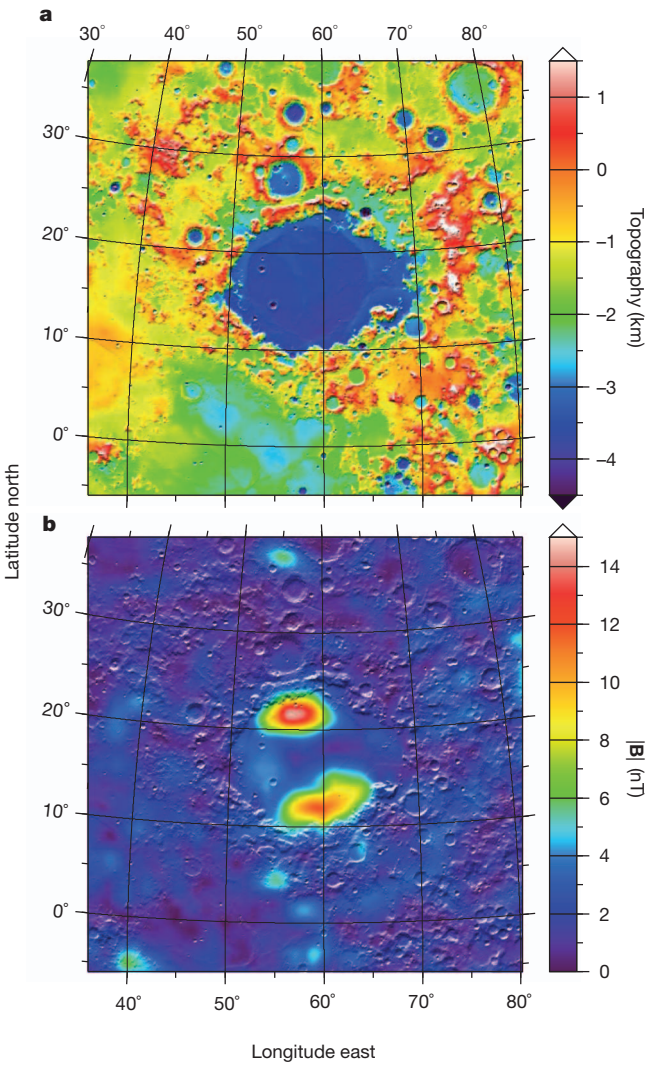

Figure 1 | Surface topography and total magnetic field strength of the ~550-km-diameter Crisium impact basin. **a**, Topography; **b**, magnetic field strength ($|\mathbf{B}|$). Two prominent anomalies are confined to the interior of this basin, where a thick impact melt sheet is predicted. The magnetic field strength is derived from the global sequential Lunar-Prospector-based model[1] evaluated 30 km above the mean planetary radius, and the topography is from the Lunar Reconnaissance Orbiter laser altimeter data[30]. Both images are displayed in a Lambert azimuthal equal-area projection with an image width and height of 1,200 km, and are overlain by a shaded relief map derived from the surface topography.

[1]IRPHE, CNRS and Aix-Marseille Université, 49 rue F. Joliot Curie, BP 146, 13384 Marseille Cedex 13, France. [2]Institut de Physique du Globe de Paris, Université Paris Diderot, 4 Avenue de Neptune, 94100 Saint Maur des Fossés, France. [3]Royal Observatory of Belgium, 3 Avenue Circulaire, BE 1180 Uccle, Belgium.

core[13] would have initially kept rotating at the pre-impact synchronous rate and would then have accelerated or decelerated much more gradually. Differential rotation at the core–mantle boundary would persist for thousands of years, potentially giving rise to hydrodynamic instabilities that could drive a core dynamo. Not only would these basin-forming impacts set up conditions under which highly magnetic impact melt rocks could acquire a thermoremanent magnetization, but they could also power a core dynamo to magnetize these rocks.

A huge amount of energy is stored in the spin and orbital motions of any planet, and under certain circumstances a portion of this energy can be used to drive three-dimensional flows in a fluid core. One mechanism for this is the excitation of hydrodynamic instabilities known as inertial instabilities. These instabilities involve a resonance between two inertial waves of the rotating fluid and a large-scale natural forcing, such as that from precession[14,15], librations[16] or tides[9] (Supplementary Information, section 1). The resulting fluid flows are highly energetic (see the demonstration in ref. 15 in response to the initial criticism in refs 17, 18) and dynamo capable, as has already been demonstrated for precession[19,20] (Supplementary Information, section 2). Regarding instabilities excited by tides (tidal instability[21]), laboratory experiments[9] have shown that a fully three-dimensional turbulent flow develops in the bulk fluid when the ratio between the equatorial ellipticity of the core–mantle boundary, β, and the square root of the Ekman number, E (which represents the ratio between viscous and Coriolis forces), is larger than a critical value of order one, and when a difference in angular velocity exists between the mean rotation of the fluid and the elliptical distortion of the fluid container. The root mean squared velocity of the flow is then of the same order of magnitude as the differential rotation[22]. In the case of the Moon, a lower-bound estimate (Supplementary Information, section 3, and Supplementary Fig. 2) gives values of β between 1.9×10^{-5} today and 1.5×10^{-4} when the Earth–Moon separation was about half of its current value, with corresponding Ekman numbers from 3×10^{-12} to 10^{-12}. The ratio $\beta/E^{1/2}$ is always greater than ten, allowing tidal instabilities to develop in the lunar core over its entire history, provided that an instantaneous non-zero differential rotation is imposed between the fluid core and mantle ellipticity.

The impact events that formed the large Nectarian-age impact basins with magnetic anomalies could all have unlocked the Moon from synchronous rotation[8] (Supplementary Information, section 3.1). Given the relatively short resynchronization timescales, the pre-impact tidal deformation of the core–mantle boundary would remain frozen in the mantle, thus providing a differential rotation, $\Delta\Omega$, between the fluid core and the elliptical distortion of the core–mantle boundary. To generate a dynamo, two additional criteria must be met (Methods and Supplementary Information, section 2): the time it takes for the tidal instability to establish a fully turbulent state must be shorter than the time it takes the core to spin up or down to the mantle rotation rate, and the core flow must be vigorous enough that the magnetic Reynolds number is larger than the threshold value for dynamo action. The characteristic amplitude of the magnetic field intensity in the core is then estimated by adapting scaling relations developed for convective dynamos[23–25] to our case of mechanical forcing. As for convective dynamos, the magnetic field strength at saturation is controlled by the available mechanical power rather than by any force balance. By assuming a turbulent core–mantle boundary layer[13,26] as well as a rapid growth of the dynamo process, the magnetic field strength at the surface of the Moon is estimated to be (Methods)

$$B \approx f[0.0026\mu_0\rho R^2(\Delta\Omega)^2]^{1/2}(R/R_{\mathrm{Moon}})^3 \qquad (1)$$

where R_{Moon} and R are respectively the mean radii of the Moon and its core, ρ is the core density, μ_0 is the magnetic constant (the permeability of free space) and f is a prefactor of order one that expresses both the efficiency of power conversion from viscous dissipation to Joule dissipation and the ratio of the dipolar component of the exterior magnetic field strength to the total core field strength. As a conservative estimate, we use $f = 0.13$ (Methods).

The expected magnetic field strength at the surface of the Moon is shown in Fig. 2 for Earth–Moon separations ranging between 25 and 55 Earth radii and for post-impact spin periods of between 3 and 35 days (see also the more detailed discussion in Supplementary Information, section 3.1, and Supplementary Figs 4–7). The Earth–Moon separation was probably less than 45 Earth radii in the Nectarian period, and the current separation is 60 Earth radii. The post-impact rotation rates following the formation of a 700-km-diameter basin with an average impact geometry are shown in red in Fig. 2 (Supplementary Information, section 3.1, and Supplementary Fig. 3). Other impact geometries, or a succession of impacts closely spaced in time, could have given rise to either larger or smaller changes in the rotation rate. In Fig. 2a, the tidal instability growth rates were calculated using the hydrostatic core–mantle boundary ellipticity. Given that the lithosphere of the Moon is not in hydrostatic equilibrium, this generates an additional gravitational potential at the core–mantle

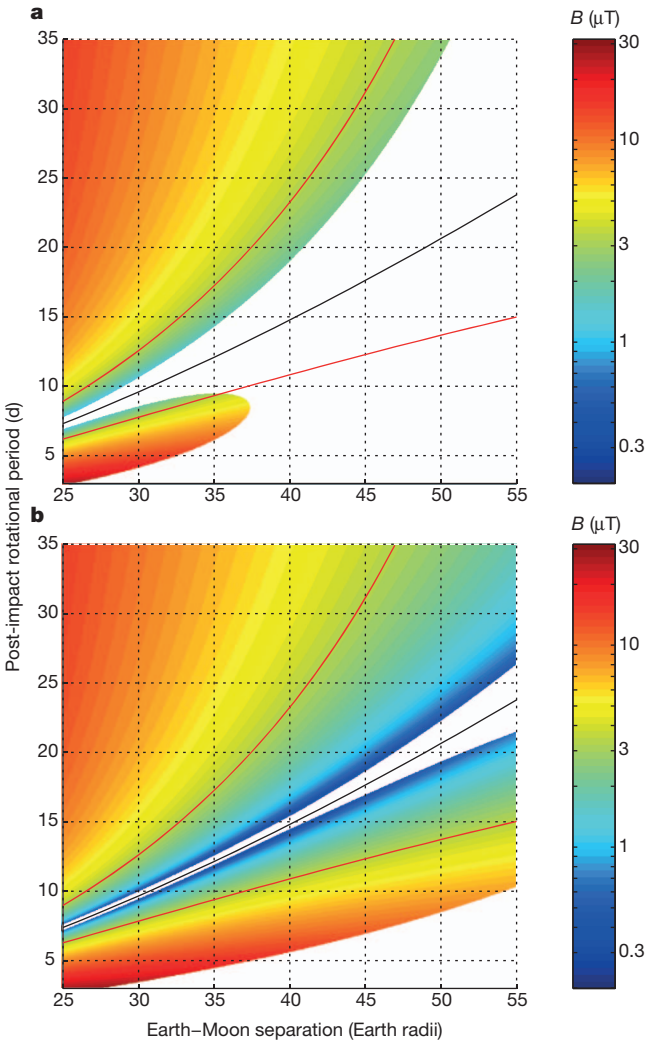

Figure 2 | Estimated magnetic field strength at the Moon's surface as a function of Earth–Moon separation and post-impact rotational period. Field strengths are plotted only when dynamo generation is possible. Also shown are the synchronous rotation rate of the Moon (black lines) and the expected range of rotational periods following the formation of a 700-km-diameter basin by a 5 km s^{-1} impact under average impact conditions (bounded by red lines; Supplementary Information, section 3.1, and Supplementary Fig. 3). The core–mantle boundary ellipticity is assumed to be equal to that of a purely hydrostatic Moon in **a**, and is assumed to be ten times this value in **b**.

boundary, causing the ellipticity to be greater than that of a purely hydrostatic Moon[27]. As an extreme case, the magnetic field strength is plotted in Fig. 2b using an ellipticity ten times larger than the purely hydrostatic value (Supplementary Information, section 3). Although the core–mantle boundary ellipticity does not affect the amplitude of the generated magnetic field at saturation, it does influence the growth rates of the tidal instability and, hence, the parameter space in which it can develop.

Dynamo action driven by tidal instabilities is possible over a large range of post-impact rotation periods and Earth–Moon separations. Predicted magnetic field strengths are significant, and range from about 0.2 to 4 μT at the surface of the Moon following the formation of a 700-km-diameter basin. These values compare favourably to those obtained from lunar palaeomagnetic analyses[5] that imply minimum field strengths of ~1 μT. Given the uncertainty of the prefactor, f, in equation (1), the actual field strengths could be up to about ten times larger. On the basis of the core spin-up times, the duration for each impact-induced dynamo is predicted to be between about 2×10^3 and 8×10^3 years, which would allow about 1 km of impact melt to cool through its Curie temperature and acquire a thermoremanent magnetization (Fig. 3). At the point where the Moon becomes synchronously locked, it would go through a phase of large-amplitude free librations, and these librations could also power a second dynamo, generating surface field strengths on the order of 1 μT (Supplementary Information, section 3.2, and Supplementary Figs 8 and 9).

Apart from forming magnetic anomalies associated with the impact melt sheets of large basins, it is also possible that impact-induced dynamos could have simultaneously magnetized portions of the proximal and distal ejecta of the basin. Magmatic intrusions and extrusive volcanic rocks that were cooling through their Curie temperatures when these dynamos were operating would have acquired a thermoremanent magnetization. Smaller impact events during this time could have magnetized crustal rocks elsewhere by the process of shock remanent magnetization[28]. Furthermore, in addition to the six Nectarian-age impact craters that possess central magnetic anomalies, other impacts could have unlocked the Moon from synchronous rotation[8], potentially powering dynamos in the Imbrian and pre-Nectarian periods. The lack of a clear central magnetic anomaly with these impact basins could be explained by either post-impact processes or differences in the abundance of magnetic carriers in the impact melt sheet.

Dynamos powered by impact-induced changes in rotation rate and subsequent tidal instabilities could thus explain a large portion of lunar magnetic anomalies and natural remanent magnetizations of lunar samples. Previous studies have also suggested the possibility of generating dynamos by tidal instabilities on Io[16] and Mars[29], and the formalism presented in this work makes it possible not only to test these hypotheses quantitatively, but to estimate the magnitude of the surface magnetic field strengths. Similar time-variable tidal deformations on Mercury, Ganymede, (early) Earth and some exoplanets could potentially account for various aspects of the magnetic fields observed with these bodies.

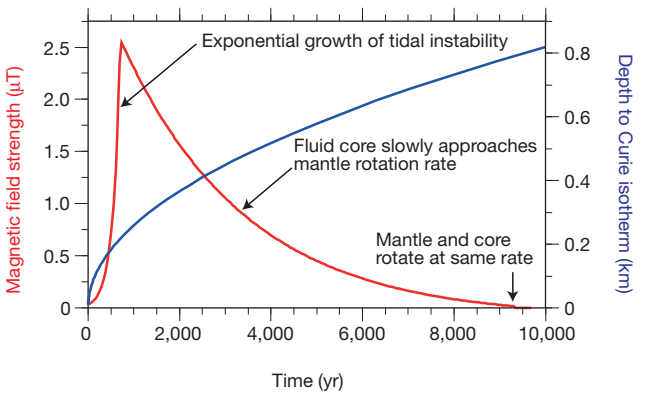

Figure 3 | Time evolution of the surface magnetic field strength (red) and depth to the Curie temperature in an impact melt sheet (blue) following an impact event. Here we consider an impact event that formed a 700-km-diameter basin at an Earth–Moon separation of 45 Earth radii. The spin period of the mantle following the impact is 31.2 days. The field strength in the exponential growth phase was estimated by assuming initial velocity perturbations in the core equal to 1% of the differential rotation and by using a core–mantle boundary ellipticity five times larger than the purely hydrostatic value.

METHODS SUMMARY

The saturation strength of the magnetic field given by equation (1) is estimated following previous works on convective dynamos. We first suppose that the ratio between the magnetic energy and the Joule dissipation is proportional to the magnetic dissipation time[23]. Following ref. 24, we then relate the Joule dissipation to the power dissipated by the elliptical instability. The mechanical power is evaluated following refs 9 and 22 by assuming that it is equal to the viscous dissipation at the Ekman boundary layer adjacent to the core–mantle boundary. This boundary layer results from the differing velocities of the fluid core and the solid mantle. This approach has been extended to account for the turbulent boundary layer expected for the Moon, following ref. 26. In plotting Fig. 2, the growth time of the tidal instability is determined for various Earth–Moon separations and spin periods of the mantle after impact using the analytical formula given in ref. 9. Also, we estimate the magnetic Reynolds number of the flow using the differential velocity between the mantle and the core. The magnetic field amplitude given by equation (1) is plotted when the magnetic Reynolds number is above the threshold for dynamo generation (estimated to be 1,000; Supplementary Information, section 2) and when the growth time of the elliptical instability is less than the core spin-up time. In Fig. 3, the time evolution of the differential rotation between the core and the mantle is calculated using a coupled numerical simulation that takes into consideration tidal and friction torques with the parameters in Supplementary Table 1. The field strength is estimated using the stationary equation (1), assuming a quasistatic evolution of a saturated magnetic field. The depth at which the Curie temperature is reached is estimated by the conductive cooling of a semi-infinite half-space.

Full Methods and any associated references are available in the online version of the paper at www.nature.com/nature.

Received 8 June; accepted 15 September 2011.

1. Purucker, M. E. & Nicholas, J. B. Global spherical harmonic models of the internal magnetic field strength of the Moon based on sequential and coestimation approaches. *J. Geophys. Res.* **115,** E12007 (2010).
2. Fuller, M. & Cisowski, S. M. in *Geomagnetism* (ed. Jacobs, J. A.) 307–455 (Academic, 1987).
3. Stegman, D. R., Jellinek, A. M., Zatman, S. A., Baumgardner, J. R. & Richards, M. A. An early lunar core dynamo driven by thermochemical mantle convection. *Nature* **421,** 143–146 (2003).
4. Lawrence, K., Johnson, C., Tauxe, L. & Gee, J. Lunar paleointensity measurements: implications for lunar magnetic evolution. *Phys. Earth Planet. Inter.* **168,** 71–87 (2008).
5. Garrick-Bethell, I., Weiss, B. P., Shuster, D. L. & Buz, J. Early lunar magnetism. *Science* **323,** 356–359 (2009).
6. Wieczorek, M. A. *et al.* The constitution and structure of the lunar interior. *Rev. Mineral. Geochem.* **60,** 221–364 (2006).
7. Hood, L. L. & Artemieva, N. A. Antipodal effects of lunar basin-forming impacts: initial 3D simulations and comparisons with observations. *Icarus* **193,** 485–502 (2008).
8. Wieczorek, M. A. & Le Feuvre, M. Did a large impact reorient the Moon? *Icarus* **200,** 358–366 (2009).
9. Le Bars, M., Lacaze, L., Le Dizès, S., Le Gal, P. & Rieutord, M. Tidal instability in stellar and planetary binary systems. *Phys. Earth Planet. Inter.* **178,** 48–55 (2010).
10. Halekas, J. S., Lin, R. P. & Mitchell, D. L. Magnetic fields of lunar multi-ring impact basins. *Meteorit. Planet. Sci.* **38,** 565–578 (2003).
11. Hood, L. L. Central magnetic anomalies of Nectarian-aged lunar impact basins: Probable evidence for an early core dynamo. *Icarus* **211,** 1109–1128 (2011).
12. Cintala, M. J. & Grieve, R. A. F. Scaling impact melting and crater dimensions: implications for the lunar cratering record. *Meteorit. Planet. Sci.* **33,** 889–912 (1998).
13. Williams, J. G., Boggs, D. H., Yoder, C. F., Ratcliff, J. T. & Dickey, J. O. Lunar rotational dissipation in solid body and molten core. *J. Geophys. Res.* **106,** 27933–27968 (2001).
14. Malkus, W. V. R. Precession of the Earth as the cause of geomagnetism. *Science* **160,** 259–264 (1968).
15. Kerswell, R. R. Upper bounds on the energy dissipation in turbulent precession. *J. Fluid Mech.* **321,** 335–370 (1996).

16. Kerswell, R. R. & Malkus, W. V. R. Tidal instability as the source for Io's magnetic signature. *Geophys. Res. Lett.* **25,** 603–606 (1998).
17. Rochester, M. G., Jacobs, J. A., Smylie, D. E. & Chong, K. F. Can precession power the geomagnetic dynamo? *Geophys. J. R. Astron. Soc.* **43,** 661–678 (1975).
18. Loper, D. E. Torque balance and energy budget for the precessionally driven dynamo. *Phys. Earth Planet. Inter.* **11,** 43–60 (1975).
19. Tilgner, A. Precession driven dynamo. *Phys. Fluids* **17,** 034104 (2005).
20. Wu, C.-C. & Roberts, P. H. On a dynamo driven by topographic precession. *Geophys. Astrophys. Fluid Dyn.* **103,** 467–501 (2009).
21. Kerswell, R. R. Elliptical instability. *Annu. Rev. Fluid Mech.* **34,** 83–113 (2002).
22. Cébron, D., Le Bars, M., Leontini, J., Maubert, P. & Le Gal, P. A systematic numerical study of the tidal instability in a rotating triaxial ellipsoid. *Phys. Earth Planet. Inter.* **182,** 119–128 (2010).
23. Christensen, U. R. & Tilgner, A. Power requirement of the geodynamo from ohmic losses in numerical and laboratory dynamos. *Nature* **429,** 169–171 (2004).
24. Christensen, U. R. & Aubert, J. Scaling properties of convection-driven dynamos in rotating spherical shells and application to planetary magnetic fields. *Geophys. J. Int.* **166,** 97–114 (2006).
25. Christensen, U. R., Holzwarth, V. & Reiners, A. Energy flux determines magnetic field strength of planets and stars. *Nature* **457,** 167–169 (2009).
26. Yoder, F. & Hutchison, R. The free librations of a dissipative Moon. *Phil. Trans. R. Soc. Lond. A* **303,** 327–338 (1981).
27. Meyer, J. & Wisdom, J. Precession of the lunar core. *Icarus* **211,** 921–924 (2011).
28. Gattacceca, J. *et al.* Unraveling the simultaneous shock magnetization and demagnetization of rocks. *Earth Planet. Sci. Lett.* **299,** 42–53 (2010).
29. Arkani-Hamed, J. Did tidal deformation power the core dynamo of Mars? *Icarus* **201,** 31–43 (2009).
30. Smith, D. E. *et al.* Initial observations from the Lunar Orbiter Laser Altimeter (LOLA). *Geophys. Res. Lett.* **37,** L18204 (2010).

Supplementary Information is linked to the online version of the paper at www.nature.com/nature.

Acknowledgements M.L.B. and D.C. acknowledge discussions with P. Le Gal and S. Le Dizès. Ö.K. acknowledges the support of the Belgian PRODEX programme.

Author Contributions M.L.B. and D.C. performed the fluid mechanics analysis, M.A.W. contributed to the analysis of the basin magnetic anomalies and post-impact rotation rates, Ö.K. contributed to analysis of the post-impact rotational evolution of the Moon and M.L. performed the impact melt thermal evolution analysis. All authors contributed to the conclusions presented in the manuscript.

Author Information Reprints and permissions information is available at www.nature.com/reprints. The authors declare no competing financial interests. Readers are welcome to comment on the online version of this article at www.nature.com/nature. Correspondence and requests for materials should be addressed to M.L.B. (lebars@irphe.univ-mrs.fr).

METHODS

Saturation strength of the magnetic field. The saturation strength of the magnetic field, B, generated by a tidal dynamo, as given by equation (1), can be estimated by adapting scaling relationships previously derived for convective dynamos to our case of mechanical forcing. Similar to refs 24, 25, we assume that the magnetic field strength in the core is controlled by the available mechanical power rather than by any force balance. For the elliptical instability considered here, we know that thermal effects to first order do not influence the amplitudes of the tidally generated flow pattern[31,32]. We thus model the core as a homogeneous, incompressible, electrically conductive fluid and neglect any thermal or stratification effects. Because precessional (and presumably tidal) dynamos do not depend on a driving thermal convection, we assume that all mechanical power that is dissipated by the instability is available for dynamo generation.

The mechanical power dissipated by elliptical instabilities has been evaluated in ref. 9 and validated numerically in ref. 22 (see equation (19) and fig. 10 therein) for the simplest form of the instability, the 'spin-over' mode, which corresponds to a rigid-body rotation of the fluid along an inclined axis with respect to the spin axis. As given by equation (5) in ref. 9, this mechanical power scales as

$$P \approx \frac{8}{3}\pi R^3 \eta \delta \Omega^2 \frac{R}{\delta} \qquad (2)$$

where $\eta = \nu\rho$ is the core dynamic viscosity (ν is the core kinematic viscosity and ρ is the core density) and δ is the Ekman boundary layer thickness, $\delta \approx R\sqrt{E}$ (see, for example, ref. 33), with an Ekman number, $E = \nu/(\Omega_{\mathrm{mantle}} R^2)$, that depends on Ω_{mantle}, the mean spin rate of the mantle. This viscous dissipation results from the differing velocities of the fluid core and the solid mantle at the laminar Ekman boundary layer adjacent to the core–mantle boundary. By neglecting the bulk turbulence that would develop in the fluid interior at the low Ekman numbers relevant for planetary cores, equation (2) gives a lower-bound estimate for the dissipated mechanical power. The dissipation of energy associated with elliptical instabilities that are more complicated than the spin-over mode will also occur mainly by viscous dissipation of kinetic energy through the Ekman layer. This means that the scaling powers in the various parameters of equation (2) should not depend strongly on the selected mode. Nevertheless, we acknowledge that a prefactor f_P, most probably larger than one, should be included in equation (2) to account for the small-scale motions associated with the more complicated instabilities.

The same expression as equation (2) is derived for the mechanical power dissipated by the precession of the lunar mantle in ref. 13 (see equations (81a) and (54) therein). This is not surprising given the similarity between the spin-over mode of the elliptical instability and the so-called Poincaré tilt-over mode excited by precession[34]. Nevertheless, it is important to emphasize that the elliptical instabilities of interest here are expected to induce motions with much larger amplitudes than the small precessional flow considered in ref. 13, where $\Delta\Omega = \Omega_{\mathrm{mantle}} \sin(I)$ with I being the (small) angle between the equatorial and ecliptic planes. Even in the limit of small-amplitude flows, a more reasonable estimate of the Moon's core–mantle friction, based on the onset of fluid turbulence in the boundary layer, should be considered[26]: in this case, the rate of dissipation depends on an 'eddy' viscosity rather than on the molecular viscosity. The problem of turbulent core–mantle coupling has still to be resolved explicitly, but a reasonable estimate is given in ref. 26 and redeveloped in ref. 13 (see equations (81a) and (55) in ref. 13), leading to

$$P \approx f_P \frac{3}{4}\pi^2 \kappa R^5 \rho |\Delta\Omega|^3 \qquad (3)$$

where κ is a constant of the order of 7.3×10^{-4} for a 350-km-radius core with a viscosity of $10^{-6}\,\mathrm{m^2\,s^{-1}}$. As introduced above, f_P is a constant of order one that is related to the complexity of the selected mode of the elliptical instability.

To estimate the magnetic field strength at saturation associated with an elliptical instability, we follow ref. 24 and relate the power, P, dissipated by the elliptical instability to the Joule dissipation, D_{ohm}, through $D_{\mathrm{ohm}} = f_{\mathrm{ohm}} P$, where f_{ohm} is a constant less than one that depends on the energy source powering the dynamo. Further supposing that the ratio between the magnetic energy

$$E_B = \frac{4}{3}\pi R^3 \frac{B_{\mathrm{core}}^2}{2\mu_0}$$

and the Joule dissipation is proportional to the magnetic dissipation time (ref. 24)

$$\frac{E_B}{D_{\mathrm{ohm}}} \propto \frac{R}{u}$$

where u is the characteristic velocity driven by the instability ($u \approx R\Delta\Omega$ for elliptical instabilities[22]), we find characteristic magnetic field strengths in the core of

$$B_{\mathrm{core,L}} \approx \sqrt{4 f_{\mathrm{ohm}} f_P \mu_0 \rho R\, |\Delta\Omega|\, \sqrt{\nu\, \Omega_{\mathrm{mantle}}}} \qquad (4)$$

for the laminar estimate of power dissipation (equation (2)) and

$$B_{\mathrm{core,T}} \approx \sqrt{\left(\frac{9\pi}{8}\right) f_{\mathrm{ohm}} f_P \kappa \mu_0 \rho R^2 (\Delta\Omega)^2} \qquad (5)$$

for the turbulent estimate of power dissipation (equation (3)). Because of the attenuation of magnetic anomalies with height, it is likely that only the dipolar component of the magnetic field will be important at the surface, which leads to a magnetic field estimate at the planet surface of

$$B \approx f_{\mathrm{dip}} B_{\mathrm{core}} \left(R/R_{\mathrm{planet}}\right)^3 \qquad (6)$$

where R_{planet} is the mean planetary radius and f_{dip} is the ratio of the dipolar component of the magnetic field strength just outside the core to the total magnetic field strength inside the core–mantle boundary. Equation (1) directly derives from the combination of equations (5) and (6). We note that the value of the ellipticity of the core-mantle boundary, β, does not appear in these formulae: the value of β determines whether or not the elliptical instability can be excited, but once the flow has developed the induced motions and magnetic field depend only on the differential rotation between the fluid core and the mantle.

Equations (4), (5) and (6) represent the most up-to-date estimate of the magnetic field strength driven by an elliptical instability, but several sources of uncertainty exist in this estimate, mainly as a result of the unknown prefactor, $f_{\mathrm{dip}}\sqrt{f_{\mathrm{ohm}} f_P}$. The efficiency factor for the conversion of mechanical power to Joule dissipation, f_{ohm}, has been estimated[24] to range between about 0.2 and 0.8 in a numerical model of convective dynamos, but it has been argued[25] that this should be closer to 0.88 for the Earth. Moreover, on the basis of magnetohydrodynamic simulations[24], and as further discussed in ref. 25, the ratio between the external dipolar magnetic field strength and the internal core field strength, f_{dip}, is about 1/7 for Earth-like convective dynamos. However, we suspect that the prefactor f_P, which is equal to one for the simple spin-over mode, could be greater than one for more-complicated flow patterns. In addition to these prefactors, the core radius of the Moon is uncertain, and a $\pm$50-km uncertainty would affect the surface magnetic field strength by a factor of about 1.6. An uncertainty of a factor of ten in the core molecular viscosity would yield an uncertainty of a factor of about 1.7 in the total field strength estimated by the laminar scaling law. And, finally, as discussed in ref. 13, various estimates for the turbulent coupling parameter, κ, lie in the range 0.0005–0.0021: with respect to our nominal value of 7.3×10^{-4}, the magnetic field strength could be uncertain by a factor of about 1.7. Considering the above uncertainties, but also claiming that the relevant physics are taken into account in the above derivation, we consider equations (4) and (5) to be precise to within a factor of order one. To provide a reliable lower-bound estimate for the surface magnetic field strength of the Moon from equation (6), we use a combined prefactor of $f_{\mathrm{dip}}\sqrt{f_{\mathrm{ohm}} f_P} = 0.13$ in our magnetic field calculations, with $f_{\mathrm{dip}} = 1/7$, $f_{\mathrm{ohm}} = 0.88$ and the restrictive value $f_P = 1$.

Growth rate of the tidal instability. After a large impact event desynchronizes the Moon's rotation, a differential rotation, $\Delta\Omega$, will exist between the fluid core and the elliptically deformed core–mantle boundary. The pre-impact elliptical shape of core–mantle boundary is assumed to remain 'frozen' into the mantle during the short time it takes the Moon to become resynchronized by tidal forces. The differential rotation can be either positive or negative depending on whether the impact accelerates or decelerates the rotation rate of the Moon, and will persist as long as the fluid core has not spun up (or spun down) to the rotation rate of the mantle. When a rotating spherical container and enclosed fluid are initially in rigid-body rotation, and when the container is suddenly set spinning with a different angular velocity, Ω_{mantle}, the mean angular velocity of the fluid will spin up or down exponentially quickly to this new rotation rate with a characteristic timescale given by[33]

$$T_{\mathrm{spin\text{-}up}} = \frac{1}{\Omega_{\mathrm{mantle}}\sqrt{E}} \qquad (7)$$

This core spin-up time should be considered approximate, as it assumes laminar flow. The development of an elliptical instability would give rise to three-dimensional fluid flows that could alter this value. The rotation rate of the mantle will progressively resynchronize with the orbital motion on a timescale given by[35]

$$T_{\mathrm{sync}} = \frac{2\Omega_{\mathrm{mantle}}\, d^6\, C}{3GM_{\mathrm{Earth}}^2 R_{\mathrm{Moon}}^5} \frac{Q}{k_2}$$

where d is the Earth–Moon separation, C is the lunar polar moment of inertia, Q is the quality factor, G is the gravitational constant, M_{Earth} is the mass of the Earth and k_2 is the degree-2 Love number. This timescale is considerably longer than the core spin-up timescale given by equation (7). Assuming a quasisteady state, where the

core spin-up time is greater than the growth time of the elliptical instability, the growth rate of the tide-driven elliptical instability can be analytically determined from the results of ref. 9:

$$\sigma_{\text{growth}} = \frac{(3\Delta\Omega + 2\Omega_{\text{mantle}})^2}{16(\Delta\Omega + \Omega_{\text{mantle}})^2}\beta|\Delta\Omega| - \alpha\sqrt{E}\Omega_{\text{mantle}} \quad (8)$$

Here α is a constant of order one that accounts for the amplitude of the viscous dissipation over the core–mantle boundary and which depends on the inertial waves that are excited. In the following, we take $\alpha = 2.62$, which is the relevant value for the spin-over mode[36]. The characteristic growth time is then simply given by $T_{\text{growth}} = 1/\sigma_{\text{growth}}$. We note that, as mentioned in ref. 9, instabilities cannot occur in a 'forbidden zone', $-3/2 < \Omega_{\text{mantle}}/\Delta\Omega < -1/2$, where no resonance involving inertial waves and tidal forcing is possible. We also note that T_{growth} is actually a lower-bound estimate for the time necessary for the turbulent flow driven by the elliptical instability to be established, because it supposes that the instability starts from a stable laminar two-dimensional rotating flow. If the core were already unstable before the impact (for instance because the effects of a previous impact have not yet been fully dissipated), the elliptical instability would saturate and generate a fully three-dimensional flow over a much shorter period than the typical growth time.

In plotting Fig. 2, we determine the growth time of the tidal instability given by equation (8) for various Earth–Moon separations and spin periods of the mantle after impact. We also estimate the magnetic Reynolds number of the flow using the differential velocity between the mantle and the core. The magnetic field amplitude given by equation (1) is plotted when the magnetic Reynolds number is above the threshold for dynamo generation (estimated to be 1,000; Supplementary Information, section 2) and when the growth time of the elliptical instability is less than the core spin-up time (equation (7)). In Fig. 3, the time evolution of the differential rotation between the core and the mantle is calculated using a coupled numerical simulation by considering core–mantle friction as well as inelastic deformations of the Moon due to the gravitational effect of Earth (see details in ref. 37). We applied a backward finite-difference scheme with the parameters in Supplementary Table 1 and the present-day k_2/Q ratio for the Moon. The core and mantle are assumed to have the same synchronous rotation before the impact. Following the impact, the rotation of the mantle is changed instantaneously. The field strength is estimated using the stationary equation (1), assuming a slow evolution of the differential rotation by comparison with the rapid growth of the dynamo and, hence, a quasistatic evolution of a saturated magnetic field. The depth to the Curie temperature of metallic iron, 1,040 K, is estimated by the conductive cooling of a semi-infinite half-space with initial and surface temperatures of 1,400 and 210 K, respectively.

31. Lavorel, G. & Le Bars, M. Experimental study of the interaction between convective and elliptical instabilities. *Phys. Fluids* **22,** 114101 (2010).
32. Cébron, D., Maubert, P. & Le Bars, M. Tidal instability in a rotating and differentially heated ellipsoidal shell. *Geophys. J. Int.* **182,** 1311–1318 (2010).
33. Greenspan, H. P. *The Theory of Rotating Fluids* (Cambridge Univ. Press, 1968).
34. Cébron, D., Le Bars, M. & Meunier, P. Tilt-over mode in a precessing triaxial ellipsoid. *Phys. Fluids* **22,** 116601 (2010).
35. Peale, S. J. in *Planetary Satellites* (ed. Burns, J. A.) 87–112 (Univ. Arizona Press, 1977).
36. Lacaze, L., Le Gal, P. & Le Dizès, S. Elliptical instability in a rotating spheroid. *J. Fluid Mech.* **505,** 1–22 (2004).
37. Correia, A. C. M. & Laskar, J. Mercury's capture into the 3/2 spin–orbit resonance including the effect of core–mantle friction. *Icarus* **201,** 1–11 (2009).